www.elsevier.com/locate/ijadhadh

Thermo-mechanical behaviors and moisture absorption of silica nanoparticle reinforcement in epoxy resins

Peerapan Dittanet, Raymond A. Pearson, Paisan Kongkachuichay

PII: S0143-7496(17)30108-2
DOI: http://dx.doi.org/10.1016/j.ijadhadh.2017.06.006
Reference: JAAD2019

To appear in: *International Journal of Adhesion and Adhesives*

Received date: 8 October 2016
Accepted date: 14 April 2017

Cite this article as: Peerapan Dittanet, Raymond A. Pearson and Paisa Kongkachuichay, Thermo-mechanical behaviors and moisture absorption of silic nanoparticle reinforcement in epoxy resins, *International Journal of Adhesio and Adhesives,* http://dx.doi.org/10.1016/j.ijadhadh.2017.06.006

Thermo-mechanical behaviors and moisture absorption of silica nanoparticle reinforcement in epoxy resins

Peerapan Dittanet[a*], Raymond A. Pearson[b], and Paisan Kongkachuichay[c]
[a]Department of Chemical Engineering, Faculty of Engineering, Center for Advanced Studies in Industrial Technology, Kasetsart University, Bangkok, 10900, Thailand
[b]Department of Material Science and Engineering, Center for Polymer Science and Engineering, Lehigh University, PA 18015 USA
[c]Department of Chemical Engineering, Faculty of Engineering, NANOTEC Center for Nanoscale Materials Design for Green Nanotechnology and Center for Advanced Studies in Nanotechnology and Its Applications in Chemical, Food and Agricultural Industries, Kasetsart University, Bangkok, 10900, Thailand

*Corresponding author: fengppd@ku.ac.th

Abstract

An investigation of the thermo-mechanical behavior of silica nanoparticle reinforcement in two epoxy systems consisting of diglycidyl ether of bisphenol F (DGEBF) and cycloaliphatic epoxy resins was conducted. Silica nanoparticles with an average particle size of 20 nm were used. The mechanical and thermal properties, including coefficient of thermal expansion (CTE), modulus (E), thermal stability (T_d), fracture toughness (K_{IC}), and moisture absorption, were measured and compared against theoretical models. It was revealed that the thermal properties of the epoxy resins improved with silica nanoparticles, indicative of a lower CTE due to the much lower CTE of the fillers, and furthermore, DGEBF achieved even lower CTE than the cycloaliphatic system at the same wt.% filler content. Equally as important, the moduli of the epoxy systems were increased by the addition of the fillers due to the large surface contact created by the silica nanoparticles and the much higher modulus of the filler than the bulk polymer. In general, the measured values of CTE and modulus were in good agreement with the theoretical model predictions. With the Kerner and Halpin-Tsai models, however, a slight deviation was observed at high wt.% of fillers. The addition of silica nanoparticles resulted in an undesirable reduction of glass transition temperature (T_g) of approximately 20 °C for the DGEBF system, however, the T_g was found to increase and improve for the cycloaliphatic system with silica nanoparticles by approximately 16 ^{o}C. Furthermore, the thermal stability improved with addition of silica nanoparticles where the decomposition temperature (T_d) increased by 10 ^{o}C for the DGEBF system and the char yield significantly improved at 600 ^{o}C. The moisture absorption was also reduced for both DGEBF and cycloaliphatic epoxies with filler content. Lastly, the highest fracture toughness was achieved with approximately 20 wt.% and 15 wt.% of silica nanoparticles in DGEBF and cycloaliphatic epoxy resins, respectively.

Keywords: Silica nanoparticles, epoxy nanocomposites, advanced materials, epoxy resins

1. Introduction

Epoxy resins are highly crosslinked polymers that are regularly used in high performance applications and industries, such as coating, electronics, automotive, aerospace and construction, because of the good adhesive, low cost, and high strength attributes [1]. However, due to the inherent brittle nature and relatively high thermal expansion of the epoxy resins, the utility of these materials can be limited in such high performance applications. To overcome the limitations, many approaches have been proposed to reinforce the epoxy systems through the use of additives such as rubbers, core-shell particles, inorganic fillers, and combinations of these fillers [2-3]. For example, soft rubbery particles are often found to be the most successful material to toughen epoxies, however, the main drawback of using such modifiers is the reduction in modulus and glass transition temperature (T_g) [4]. Unlike rubber particles, inorganic or rigid fillers, such as silica particles, have been found to be effective reinforcing agents for thermosetting resins. Therefore, silica and silicate particles are often added as a second phase material to improve thermal and mechanical properties of epoxy resins such as stiffness, toughness and thermal expansion without the loss of modulus [5-6].

Recent developments in nanotechnology have recognized the distinct size effect of microscale and nanoscale inorganic particles towards the behavior of epoxy resins [7-8]. In particular, it was reported that nanoparticles can improve the stiffness of polymers more dramatically than micro-fillers. Furthermore, the increase of specific surface area and filler content of the nanoparticles enhances the mechanical and impact properties of composites. However, when the size of fillers becomes smaller and the loading of fillers become higher, the viscosity of composite resin will be difficult to process. Therefore, the interfacial strength becomes an important factor due to the increased surface area of fillers. Similarly, other studies have reported a considerable improvement of the mechanical [8] and thermal properties of polymer nanocomposites even at very low filler volume content. In addition to the size effect of fillers, the performance of epoxy resins is also strongly influenced by other various environmental factors, such as moisture. Moisture absorbed into a polymer can lead to unwanted expansion and reliability failure behaviors in the polymer, such as stress cracking and delamination [9-10]. Such moisture and temperature induced failures have long been recognized as an important issue for package reliability but there is often a lack of reliable material data. While these studies offer key differences in filler size, the use and understanding of nanoparticles in a polymer matrix and the surroundings warrants additional studies. Ultimately, the basic question is how the polymer properties change with incorporation of very small particles, especially on the nanometer scale.

Models for coefficient of thermal expansion (CTE) and other mechanical properties have been developed to predict and fit the experimental data. The models will be briefly introduced below, followed by a more thorough review of the models in the results and discussion section. For CTE, the recognized models include the Rule of Mixture (ROM) and the Kerner model [11-12]. The ROM has been widely used to predict the effective CTE for composites [13], however, the ROM expressions do not consider the interface interaction between the filler and polymer matrix. The Kerner model, on the other hand, estimates the CTE of the composite based on the bulk modulus of the filler and matrix. The measured CTE of the composite is found to be in good agreement with theoretical equations, such as the self-consistent method, studied by Shin and Lee [14]. For other mechanical properties, for instance modulus, the adopted models include the rule of mixture, Hashin-Shtrikman's bounds, Mori-Tanaka [15], and Halpin-Tsai [16]. The Halpin-Tsai model has been found to give good prediction for carbon nanotube, nanoclay, and nanosphere silica in nanoscale at low volume content of fillers [17-20]. However, as the filler contents increases, the predicted modulus is found to underestimate the experimental results [21]. In this study, the Kerner and Halpin-Tsai models were evaluated for the CTE and stiffness, respectively, for silica-filled epoxy systems.

Underfill epoxy resins are heavily used in the electronics industry which are added between the silicon chip and the printed circuit boards (PCB) to provide extra rigidity with strong mechanical bonding at the connectors, protect solder joints from mechanical stress, help transfer heat away from the chips as a heat sink, and act as a CTE absorber and stress-reducing agent for systems with thermal mismatch [22]. Therefore, selecting an appropriate underfill epoxy resin will depend on the chemical, mechanical, and thermal requirements, and as a result, the CTE, glass transition temperature, stiffness and other properties of the underfill must be balanced to meet the demands in this system. The general guidelines for the requirements of each property for underfill are: a) low CTE and high glass transition temperature to ensure dimensional stability over the service temperature range, b) high modulus to prevent large residual stress build up, and c) low moisture absorption to retain adhesion after exposure to humidity.

In this work, the impact of silica nanoparticle fillers on two different types of epoxy resins, namely diglycidyl ether of bisphenol F (DGEBF) and cycloaliphatic epoxy, were studied. The investigation aims to evaluate both epoxy resin systems for the coefficient of thermal expansion (CTE), modulus, toughness, thermal stability, and moisture absorption. The experimental results are compared against the Kerner model for CTE and the Halpin-Tsai model for the stiffness of particulate composites. The results of these studies will provide a fundamental understanding of fillers in epoxy resins at the nanoscale and help to design resin composites with improved mechanical and thermal properties.

2. Experimental

2.1 Materials and sample preparation

The epoxy resins used in this study were standard diglycidyl ether of bisphenol F (DGEBF, DOW Chemical Company) and 3,4-Epoxycyclohexylmethyl-3,4-epoxycyclohexanecarboxylate (cycloaliphatic epoxy, DOW Chemical Company). The two commercial resins were selected and compared based on their distinctly different molecular structures. The silica nanoparticles were commercially surface modified by a sol-gel process using an organosilane-coupling agent with an average particle size of approximately 20 nm (Hanse Chemie, Geesthacht, Germany) and were obtained at 40 wt.% concentrations in epoxy resins. 2-ethyl-4-methylimidazole (2-4 EMI, Sigma-Aldrich) and hexahydro-4-methylphthalic anhydride (Anhydride, Sigma-Aldrich) were used as curing agents for the DGEBF and cycloaliphatic epoxy resins, respectively. The chemical structures of each epoxy resins are presented as follows:

Table 1. Chemical and physical properties of the model epoxy systems [22].

Epoxy systems	Curing agents	Epoxy equivalent weight, EEW (g/mole)	Viscosity @ 25^oC (MPa*s)
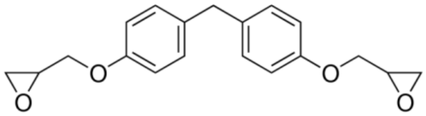 DGEBF	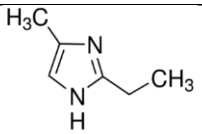 2-4 EMI	165	4000-6000
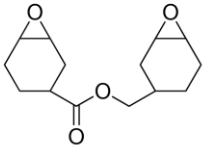 Cycloaliphatic	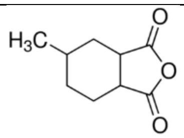 Anhydride	131-143	350-450

The formulations for DGEBF were carried out by mixing an appropriate amount of epoxy resin with concentrations between 0-35 wt.% of silica nanoparticles for 2 h under vacuum. 4 phr of 2-4 EMI curing agent was added into the mixtures and then agitated under vacuum for 5 mins. Afterwards, the mixtures were placed on a silicone mold and thermally cured initially at 60 ^oC for 4 h and then at 150 ^oC for 2 h in air. The samples were made in the mold to the testing dimensions. The cured epoxies were gradually cooled to room temperature before the samples were released from the mold. The same general procedures were followed for cycloaliphatic epoxies except that the stoichiometric ratio of cycloaliphatic epoxy and anhydride curing agent was 1:1 with curing conducted at 125 ^oC for 3 h, followed by 200 ^oC for 1 h. Cycloaliphatic epoxies were prepared with silica nanoparticle concentrations between 0-20 wt.%.

2.2 Characterizations

2.2.1 Coefficient of thermal expansion

The coefficient of thermal expansion (CTE) of the cured materials were determined by thermal mechanical analysis (TMA, TA Instruments TMA-2940). The samples were cut to dimensions of 3 mm x 3 mm x 3 mm. The experiments were conducted from 25-200 ^oC at 1

^{o}C/min. The CTEs of glassy and rubbery states were taken from the slope of thermal expansion-temperature curves at below the glass transition temperature (T_g) and above T_g, respectively.

2.2.2 Modulus

The storage modulus, *E'*, was measured in a 3-point bending mode using a Dynamic Mechanical Analyzer (DMA, TA Instruments DMA2980). The specimens, with sample dimensions of 13 mm x 54 mm x 3 mm, were tested at a constant frequency of 1 Hz and at a temperature range from 30 to 200 ^{o}C at a heating rate of 5 ^{o}C/min.

2.2.3 Thermal stability

The thermal stabilities of the cured samples were determined by thermogravimetric analysis (TGA, TA Instruments TGA2950). Approximately 30 mg of sample was placed in an alumina dish and measured from 25-600 ^{o}C at 10 ^{o}C/min. The decomposition temperature, T_d, was considered at 10% weight loss, and the extent of char residue was compared at 600 ^{o}C. Weight loss against temperature was determined under nitrogen at a flow rate of 56 cm^3/min.

2.2.4 Fracture toughness

The plane strain fracture toughness (K_{IC}) was measured using a single-edge notch (SEN) test (Instron model 5567), in accordance with the ASTM D5045 standard. A pre-crack was made by lightly tapping a fresh razor blade between the adjoining plates, with sample dimension of 75.6 mm (h) x 12.7 mm (w) x 6.36 mm (t), yielding a very sharp natural crack. The tests were performed at a rate of 1 mm/min. The average and standard deviation values were reported with at least five samples for each composition. K_{IC} was determined using the relationship in the following equation [23]:

$$K_{IC} = Y \frac{6 P_f S}{4 t w^2} \sqrt{a} \tag{1}$$

where Y is the shape factor, P_f is the load at break, S is the length of the span (50.8 mm), t is the thickness of the sample, w is the width of the sample, and a is the crack length.

2.2.5 Moisture uptake

The cured materials were subjected to temperature and humidity aging at 85 ^{o}C and 85% relative humidity, respectively, using an ECOSPHERE humidity chamber. The water absorption was determined by measuring the increased weight gain due to moisture uptake. Prior to the measurements, the specimens were removed from the chamber and manually dried to remove moisture from the exterior surface. The average measurements with standard deviations were reported from three specimens with dimension of 10 mm x 20 mm x 3 mm for each composition.

3. Results and discussion

3.1 Glass transition temperature and coefficient of thermal expansion

The CTE values of the modified epoxies were calculated from the slopes of the data points 50 ^{o}C below and above the critical T_g value, representing glassy and rubbery states, respectively. CTE values for below and above the T_g of silica-reinforced DGEBF and cycloaliphatic epoxies are shown in Table 2. The CTE clearly decreases with increasing wt.% of silica particles for all filled epoxy systems. The decrease in CTE at higher filler fractions is due to a correspondingly lower CTE of the silica nanoparticle fillers compared to the base epoxy resins. Comparing the CTE with the type of epoxy, DGEBF versus cycloaliphatic, at the glassy and rubbery states, the CTE for the DGEBF system was revealed to be lower than cycloaliphatic at the same weight % filler content. It is likely that the lower DGEBF CTE values arise from the higher packing density in the system and is, therefore, one desirable characteristic of DGEBF in industrial applications.

Table 2. Thermal properties of silica filled DGEBF and cycloaliphatic epoxies.

Epoxy System	Wt % Fillers	T_g (^{o}C)	T_d (^{o}C)	Char Residue (%)	CTE (ppm/^{o}C)		Modulus (GPa)
					Below T_g	Above T_g	
DGEBF	0	151.8	440.2	20.9	67.3±2.0	169.0±2.0	2.30±0.10
	5	143.6	443.6	19.3	65.7±2.0	158.0±1.5	2.59±0.26
	10	136.8	444.2	25.5	64.6±1.6	147.0±1.6	3.04±0.15
	20	131.9	445.6	35.2	60.5±1.4	146.0±1.5	3.21±0.24
	30	131.3	448.6	48.3	56.3±1.5	133.0±1.0	3.43±0.12
	35	139.5	450.0	52.9	51.5±2.0	117.0±0.5	3.99±0.20
Cycloaliphatic	0	140.5	378.1	0.2	75.5±1.0	189.0±1.5	2.06±0.08

1	141.4	380.6	1.3	73.5±2.0	188.0±1.0	2.32±0.12
5	147.8	379.7	4.9	66.1±1.7	183.0±2.0	2.42±0.15
10	145.4	381.3	9.9	67.9±1.8	173.0±1.0	2.56±0.10
15	146.9	380.1	14.8	60.0±1.5	162.0±2.0	2.60±0.19
20	156.4	378.2	19.6	55.6±1.9	147.0±2.0	2.96±0.16

TMA also measured the glass transition temperature of modified epoxies, presented in Table 2 for the corresponding wt.% silica nanoparticle concentrations. The T_g values decrease with the addition of silica nanoparticles for the DGEBF systems from ~ 152 to ~131 ^oC for 0 to 30 wt.%, respectively, which suggest that silica nanoparticles have a strong impact on the T_g. The covalent bonding of the organosilane and epoxy on the surface interface of silica nanoparticles leads to an additional constraint on the system, whereby increasing an amount of cooperatives required for segmental molecular motion [24]. In addition, for DGEBF epoxy cured imidazole, the imidazole molecule can act as a chain end group, reducing the length of each polymerizing chain, and resulting in more free volume and lower crosslink epoxy [25]. Therefore, the decrease in T_g with nanocomposites may be attributed to the plasticizing effect from silica nanoparticles in the DGEBF matrix, resulting in more free volume of the epoxy resins. The plasticizing effect is particularly useful for polymer processing where fillers are added to lower the T_g, however, for epoxy systems, a higher T_g is generally preferred to enhance thermal capability. At 35 wt.% fillers, the T_g slightly increases to ~140 ^oC, which could be attributed to the reduced interparticle distance of the silica particles. Zhang et al. suggested that the physical properties of a filled epoxy can be enhanced when the interparticle distance is smaller than the nanoparticles [26]. Under this condition, the interface may construct physical networks which dominate the performance of these nanoparticles. This physical network can restrict the chain mobility of the epoxy matrix which increases the T_g. The T_g values of the cycloaliphatic system, on the other hand, are improved with silica nanoparticles. The T_g increases from 140 to 156 ^oC for 0 to 20 wt.% fillers, respectively. This result suggests that the motion of the cycloaliphatic epoxy chain is heavily inhibited by the silica domains. By comparing the molecular structure of these two epoxy systems, the DGEBF has a stiff backbone structure of aromatic rings while the cycloaliphatic system contains a structure with flexible chains. Therefore, with addition of silica, the effectiveness of the increase in free volume is more prominent with the non-cycloaliphatic systems. Chain mobility of such epoxies is much less than that of cycloaliphatic which only has alkane rings in the structure. The plasticizing effect does not have a significant impact on the cycloaliphatic system due to these molecular properties.

3.2 Modeling for CTE

Several models have been presented in the literature to model the CTE of composite systems. The Rule of Mixtures (ROM) has been widely adopted to predict the effective coefficient of thermal expansion (CTE) for composites [13]. However, the ROM expressions do not consider the interface interaction between the filler and polymer matrix. Wong et al. reported that the CTE prediction from the ROM model is much higher than experimental results [27]. Vo et al. proposed the CTE model of polymeric composites by considering the effect of an interface zone surrounding the filler particles in a polymer matrix [21]. The CTE model has been found to resolve several conflicts regarding the effect of filler concentration, filler size, and filler-polymer interaction. However, the model prediction can only be effective for their specific filler-polymer system in micro-scale and for very low filler concentration.

A model proposed by Kerner and coworkers [11], is the most commonly applied model for CTE prediction. The Kerner model estimates the CTE of the composite based on the bulk modulus of the filler and matrix. The measured CTE of a composite is found to be in agreement with experimental results studied by Shin and Lee [14], and is currently being examined by researchers for thermal and mechanical properties of polymer composites with nanoscale reinforcement [28-29]. In this model, it is assumed that the composite consists of spherical particles dispersed in the matrix and is wetted by a uniform layer of the matrix. The composites are assumed to be macroscopically isotropic and homogeneous. The model gives the CTE of a composite as [11];

$$\alpha_c = \alpha_m V_m + \alpha_f V_f + (\alpha_f - \alpha_m)\, V_m V_f \left(\frac{\frac{1}{K_m} - \frac{1}{K_f}}{\frac{V_m}{K_f} + \frac{V_f}{K_m} + \frac{3}{4G_m}} \right) \tag{2}$$

where the coefficients of thermal expansion of the composite, polymer matrix, and filler are α_c, α_m, and α_f, respectively. The bulk moduli for the polymer matrix and filler are K_m and K_f, respectively, and G_m is the shear modulus for the polymer matrix. The volume fractions are V_m and V_f for polymer matrix and filler, accordingly. It is noted that the relationship between K and G is given by the following standard expression:

$$K = \frac{E}{3\left(3 - \frac{E}{G}\right)} \qquad (3)$$

where E is the Young's modulus. The properties of epoxy matrix and silica nanoparticles used in the model prediction are given in Table 3. The densities of epoxy (DGEBF and cycloaliphatic) and silica nanoparticles used to calculate volume fractions are 1.2 and 1.93 g/cm^3, respectively [29]. The bulk moduli of epoxy matrix and fillers are calculated using equation 3. The values for α and G are obtained from experimental results as shown in Table 2.

Table 3. Material parameters used in CTE and E model predictions.

Parameters	Symbol	Values	Reference
Bulk modulus of silica nanoparticle, GPa	K_f	35.4	Eq. 3
Shear modulus of silica nanoparticles, GPa	G_f	29.9	[29]
Young's modulus of silica nanoparticles, GPa	E_f	70.0	[29]
Young's modulus of DGEBF, GPa	$^{DGEBA}E_m$	3.0	Experiment*
Young's modulus of cycloaliphatic, GPa	$^{Cyclo}E_m$	2.7	Experiment*
CTE of silica nanoparticles, ppm/^{o}C	α_f	0.55	[29]

Experiment* = Values were obtained by tensile test using dog-bone specimen (Type V), according to ASTM D638 at a displacement rate of 5 mm/min.

In the current study, the Kerner model was applied and found to predict well for selected epoxy systems. Figures 1 and 2 show the correlation between the measured CTE data points and predicted CTE by the Kerner model for the glassy states. Interestingly, at the glassy state, the estimated values for CTE correlate well over the full range of silica particle concentrations for the DGEBF and cycloaliphatic epoxies, however, the model slightly deviates at higher silica contents. In the current study using 20 nm fillers, the Kerner model predicts the experimental results well up to 20 vol% filler for DGEBF and 10 vol% filler for cycloaliphatic, but slightly deviates at above 12% filler of only the cycloaliphatic system. This deviation at high filler content is likely attributed to 1) organosilane interface layer thickness surrounding the spherical nanoparticles and 2) its interaction to the different epoxy matrices. The impact of thickness mentioned here is specifically the physical interaction by organosilane at the SN interface. For instance, in diglycidylether of bisphenol A (DGEBA) cured piperidine systems, the Kerner model for the CTE was found to fit only silica particle sizes above 74 nm and up to 30 vol% filler content, but not particularly well for the 23 nm filler (overestimation by the model for CTE), which is explained by the large area of interface as the particle size is reduced [28-29]. Furthermore, Zhang et al. [26] suggested the critical thickness of the interface where the enhanced properties are pronounced is at silica nanoparticle contents up to 23 wt.% (14 vol.%). Above this condition, where the critical thickness is reached, the interparticle distance is reduced to the range of the particle radius, and the silica nanoparticles constrains more epoxy matrix. Hence, under this condition at higher filler content, a greater decrease in CTE of the epoxy can be expected, which was unfortunately not accounted for in the Kerner model and led to the overestimation at high filler contents. Therefore, while the Kerner model can generally predict well for most selected systems, the organosilane interface layer thickness and its interaction to the epoxy matrix can play an important role when employing nanosized fillers and should be considered in the model parameters.

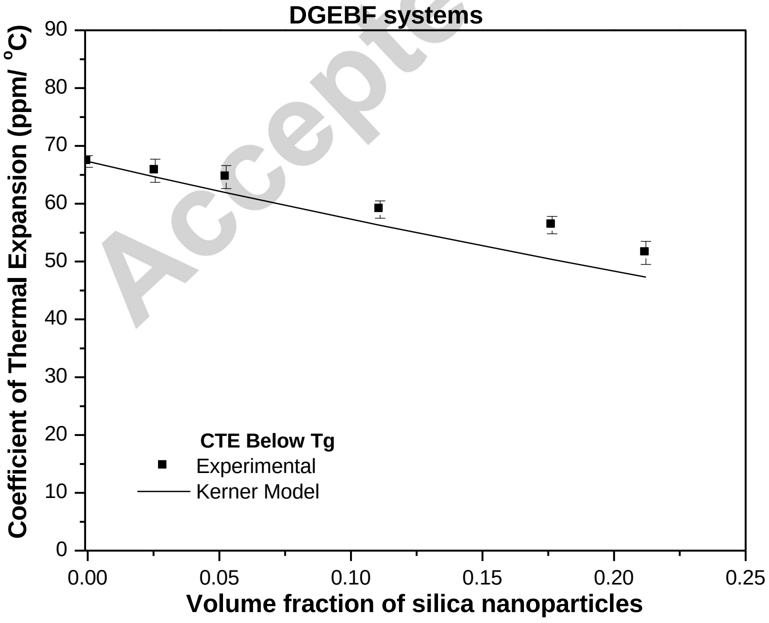

Figure 1. Coefficient of thermal expansion (CTE) at below T_g (glassy state) versus volume fraction of silica nanoparticles for DGEBF epoxy resin.

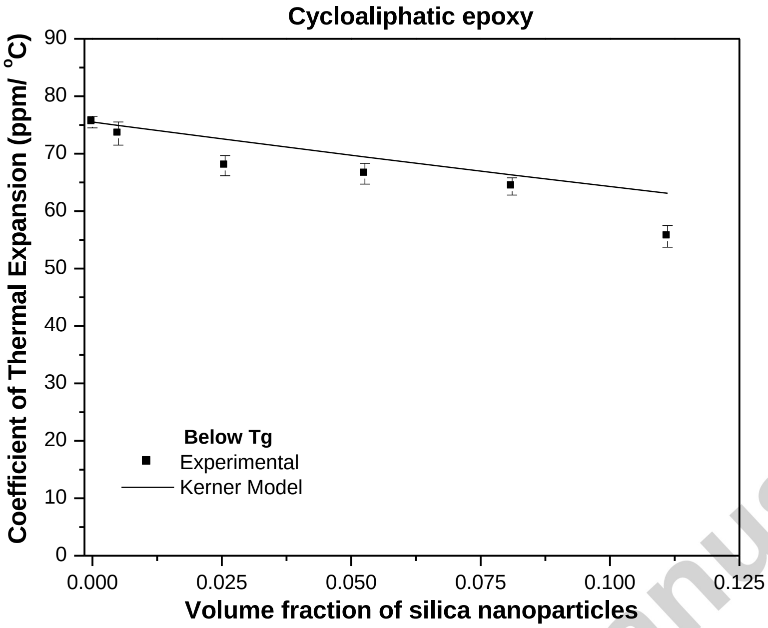

Figure 2. Coefficient of thermal expansion (CTE) at below T_g (glassy state) versus volume fraction of silica nanoparticles for cycloaliphatic epoxy resin.

3.3 Modulus

DMA measures the response of a given material to an oscillatory deformation as a function of temperature. The three parameters provided by DMA, namely storage modulus (*E*'), loss modulus (*E*''), and tanδ (*E*''/*E*'), are useful for determining the occurrence of molecular mobility transitions, such as the glass transition temperature (T_g). The modulus as a function of temperature for silica-toughened composites of DGEBF and cycloaliphatic epoxies are shown in Figures 3 and 4, respectively, and listed in Table 2. Two features are observed. Firstly, the enhancement of the storage moduli for all the filler systems at various silica particle contents can be clearly observed within the measured temperature range when compared to the neat epoxy resin, which is consistent with literature reports [29, 31]. This enhancement indicates that the silica nanoparticles have a strong effect on the elastic properties of epoxy resins. With a much higher modulus of the filler than the bulk polymer plus the large, exposed surface contact to the polymer, the significant increases in the modulus with very low filler content were undoubtedly found. This phenomenon can also be attributed to the coefficient of thermal expansion between the matrix and the particles. The CTE of the bulk silica is much lower than the CTE of the epoxy resin, resulting in a residual compressive stress between the two phases. Therefore, an increase in the modulus of epoxy resins can be expected. Secondly, the intensity of tanδ does not stay consistent with fillers, but rather, decreases with increasing filler concentration, which suggests that the fillers promote the damping of the tanδ intensity [30]. For both DGEBF and cycloaliphatic epoxies, the tanδ are clearly improved with addition of silica nanoparticles which can also be explained by restricted chain mobility in epoxy systems with the presence of silica nanoparticles.

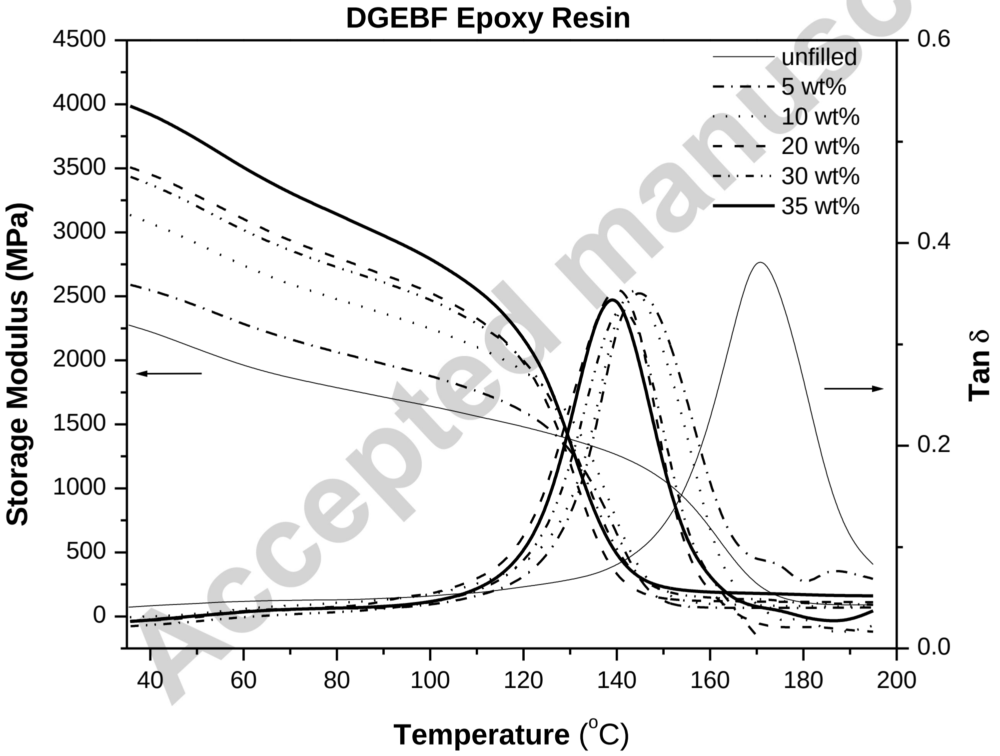

Figure 3. Dynamic mechanical analysis data for DGEBF, showing the storage modulus and tanδ versus temperature at various silica nanoparticle contents.

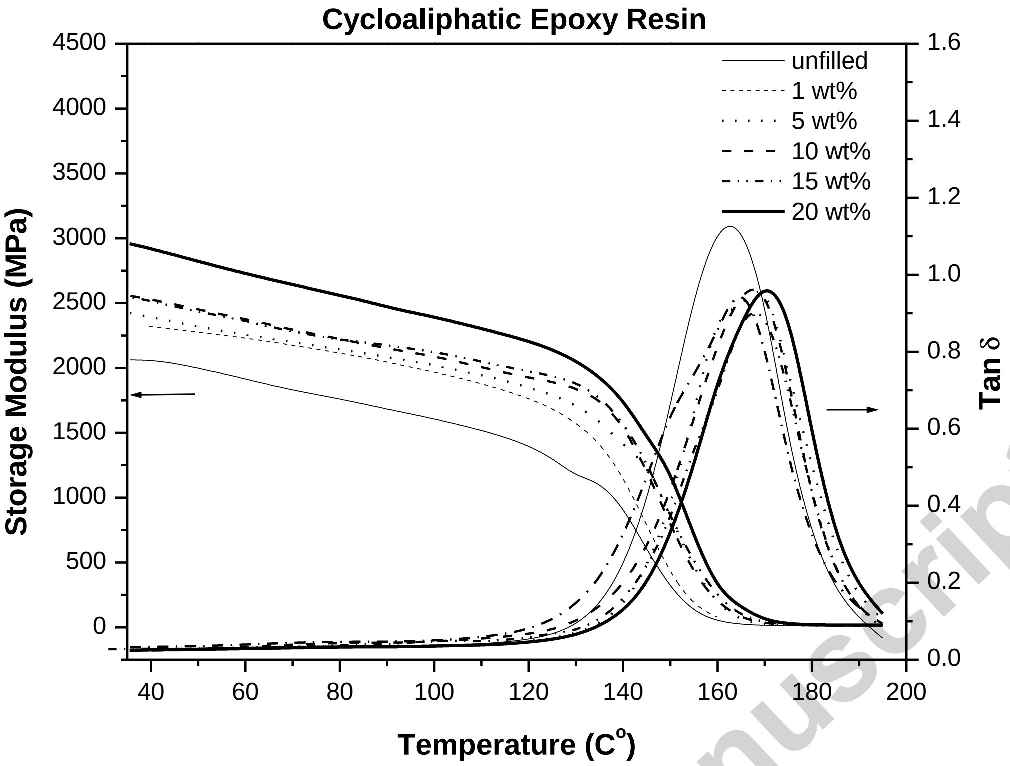

Figure 4. Dynamic mechanical analysis data for cycloaliphatic epoxy, showing the storage modulus and tanδ versus temperature at various silica nanoparticle contents.

3.4 Modeling for *E*

Predicting the mechanical properties of nanocomposites is also a challenge, and many theoretical models have been proposed to predict the properties of polymer with incorporation of fillers [20]. These models include the rule of mixture, self-consistent method, Hashin-Shtrikman's bounds, Mori-Tanaka, and Halpin-Tsai [12, 15, 16]. These models were initially developed for the elastic moduli of epoxy molding compounds (EMC) with silica particles where the matrix and the particles were assumed to be linear-elastic, isotropic, and perfectly bonded. When applying these models to nanocomposite systems, the results were not consistent, where for instance, the rule of mixture was usually found to give poor estimations. The self-consistent method and Hashin-Shtrikman's bounds were found to only be applicable at a specific system where the particles were well distributed in polymer matrix [14]. Tandon and Weng reported that the Mori-Tanaka model worked best only for particles with high aspect ratios and particles which were perfectly aligned in the composites [20]. At high aspect ratios, the reinforcing effect can be negligible, however, in nanocomposite systems, the reinforcing effect exists and cannot be neglected. Therefore, these models cannot be directly applied for nanocomposite systems.

Currently, the most widely used model is the Halpin-Tsai model, which was developed by Halpin [16]. This model takes into consideration the modulus of the composite as a function of filler content, specifically, the modulus of filler, the modulus of epoxy matrix, as well as the aspect ratio by the incorporation of a shape factor. The Halpin-Tsai model is expressed by the following equation for modulus of composites:

$$\frac{E_c}{E_m} = \frac{1 + \xi\eta\phi}{1 - \eta\phi} \qquad (4)$$

where E_c and E_m are the moduli for composite material and polymer matrix, respectively. ϕ is the filler sphere volume fraction, and η is expressed by:

$$\eta = \frac{\left(\frac{E_f}{E_m}\right) - 1}{\left(\frac{E_f}{E_m}\right) + \xi} \qquad (5)$$

where E_f is the modulus of the filler and ξ is the shape factor. The value of the shape factor relates to the geometry or the aspect ratio (width/thickness) of the fillers. For spherical particles with an aspect ratio of $a = 1$, Halpin and Kardos [33] suggested that the shape factor of $\xi = 2a$ is appropriate for predicting the modulus of a filled polymer. By taking into consideration the modulus of the composite as a function of filler content (matrix and reinforcing phases together) as well as the shape factor, the Halpin-Tsai model is particularly versatile.

Figs. 5 and 6 depict the fit of the Halpin-Tsai model to the experimental data points for the modulus versus volume fraction of fillers. The Halpin-Tsai model for the cycloaliphatic epoxy system appears to correlate well to the measured results. For the DGEBF epoxy system, the model predicts the experimental values well at low filler content. However, at high filler content, the measured moduli for the DGEBF epoxy system lie slightly below the predicted values. Similar observations have been reported in the literature for nanoclay, carbon nanotubes, and nanosphere silica at low volume content of fillers [17, 18, 32, 33]. As the filler content increases, the predicted modulus has been found to underestimate the experimental results. At low volume fractions of fillers, the model assumes perfect bonding between the particle and the polymer matrix and ignores any particle-particle interactions. However, at high volume fractions of filler, particle-particle interactions cannot be neglected. Similar results have been observed for CTE prediction of DGEBF, which suggests that particle-particle interaction at the interface could play a role.

For a spherical silica filled epoxy system, Adachi et al. [34] suggested that an enhanced mechanical property was due to a reduced interparticle distance. Based on the assumptions for cubic distribution and ideal dispersion, the relationship between the interparticle distance (τ) and the filler content (φ_p) is predicted by the following equation [34]:

$$\tau = d\left[\left(\frac{\pi}{6\varphi_p}\right)^{1/3} - 1\right] \qquad (6)$$

where d is the particle diameter. As the filler content increases, the interparticle distance of silica nanoparticles deceases. For example, comparing 5 vol% and 15 vol% silica nanoparticles with nominal 20 nm particles, τ is approximately 23.7 nm and 14.7 nm, respectively. The impact of interparticle distance on mechanical performance is more substantial when the particle size decreases from the micron to the nanometer length scale. Due to the surface modification occurring during the formation of silica nanoparticles, strong interactions at the interface between nanoparticles and polymer chains are expected. Therefore, with increasing filler content, the silica nanoparticles are packed closer together and form a core-shell configuration structure where the silica nanoparticles are coated with polymer chains at the interface.

It is likely that there is a critical filler content where the interparticle distance is reduced to the size that is much smaller than the nanoparticles [26]. Under this condition, the polymer matrix is significantly perturbed by the fillers surrounding at the interface and the perturbed region is at the same length scale. The model assumes only two phases exist in the system and does not take into account the interface. Therefore, an overestimation of the model can be expected at high filler contents when filler content reaches a critical value.

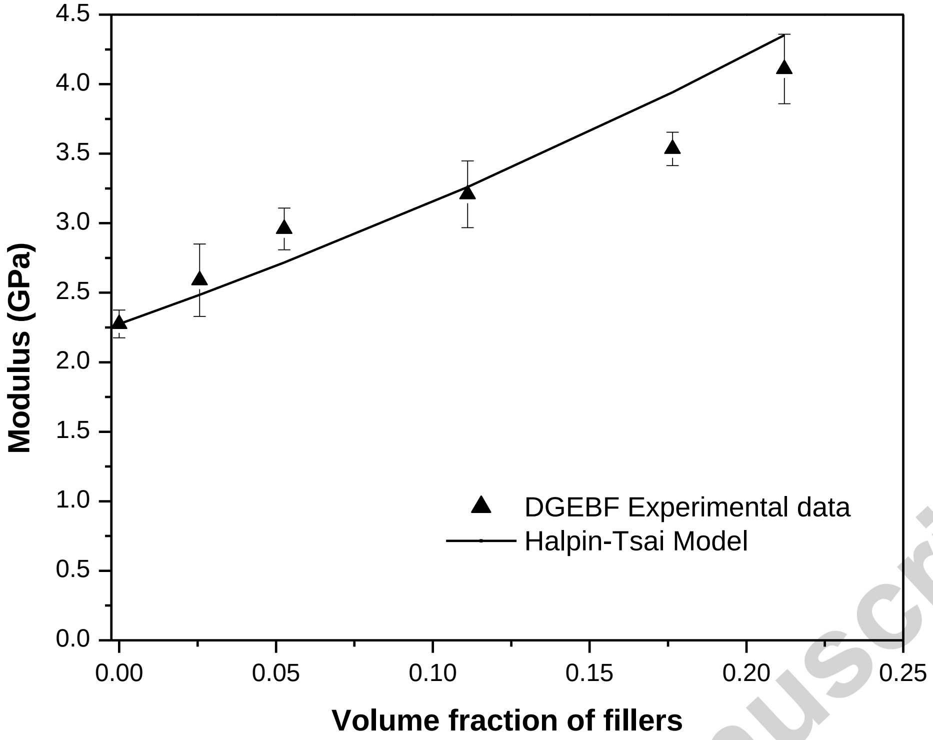

Figure 5. Modulus versus silica nanoparticles content. Points are experimental data, and solid line is the predicted data from Halpin-Tsai model for DGEBF epoxy resin.

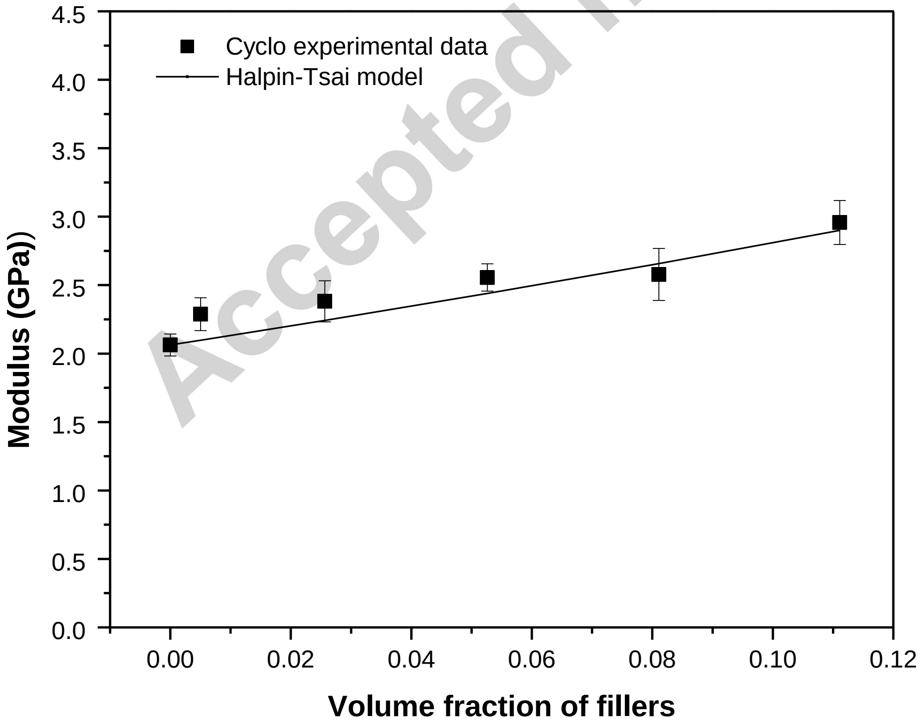

Figure 6. Modulus versus silica nanoparticles content. Points are experimental data, and solid line is the predicted data from Halpin-Tsai model for cycloaliphatic epoxy resin.

3.5 Thermal stability

The thermal stability of the epoxy resins was studied by thermogravimetric analysis (TGA). Plots of % weight as a function of temperature for the silica nanoparticle-filled DGEBF and cycloaliphatic epoxy resins are shown in Figures 7 and 8, respectively. The weight loss is due to the formation of volatile products after degradation at high temperature. The temperature at the onset of weight loss or decomposition temperature at 10% weight loss (T_d) and char residuals at 600 ^oC of the DGEBF and cycloaliphatic epoxies are summarized in Table 2. The T_d values of the DGEBF with the incorporation of silica nanoparticles are found to be higher than the neat resin and increased at higher filler concentration, indicating a higher decomposition temperature with fillers. The T_d of the cycloaliphatic epoxy, on the other hand, increases with fillers up to 10 wt.%, then decreases slightly above 15 wt.% of silica nanoparticles. The increase of T_d demonstrates that the thermal stability of the epoxy resins improves with filler addition and is proportional with the amount of loading. Furthermore, the less overall weight loss with increasing filler content from char yield correlates to improved flame retardance [31, 36].

Lee and Ma [36] suggested that a decrease in crosslink density can lead to the lowering of T_d. Therefore, it can be inferred that the decrease in T_d above 15 wt.% of nanofilled cycloaliphatic epoxy is likely attributed to the decrease in crosslink density. This result also confirms the decrease in fracture toughness of the cycloaliphatic system at filler contents above 15 wt.%, to be further discussed below. However, this phenomenon does not occur in the DGEBF system. Some researchers [35, 37] have indicated that the increase in stability is due to the improved barrier properties of the composites, where the inorganic phase can act as a radical sink to prevent polymer chains from decomposing.

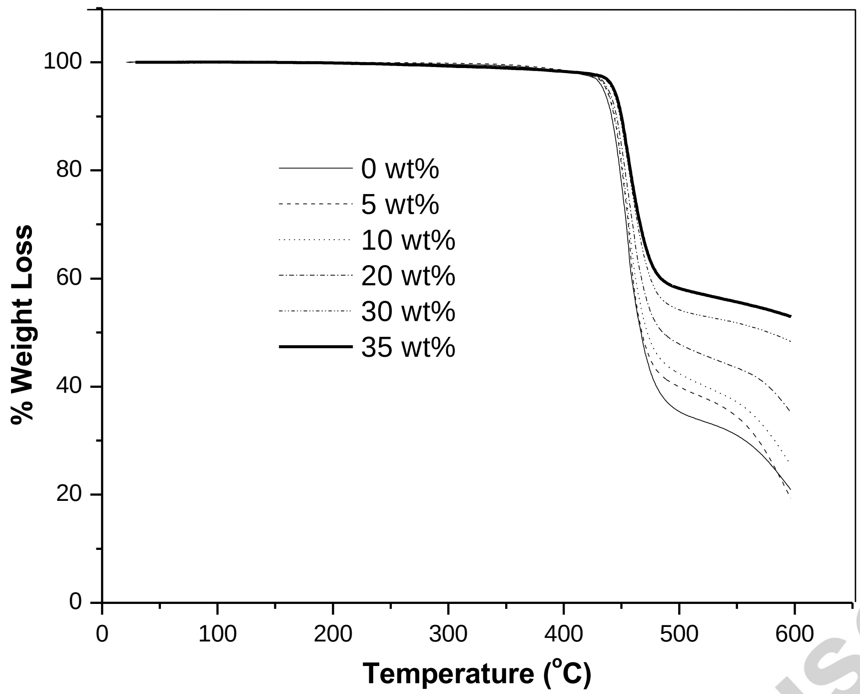

Figure 7. TGA analysis of DGEBF epoxy filled silica nanoparticles at various filler contents under N_2 atmosphere from 25 °C to 600 °C with heating rate of 10 °C/min.

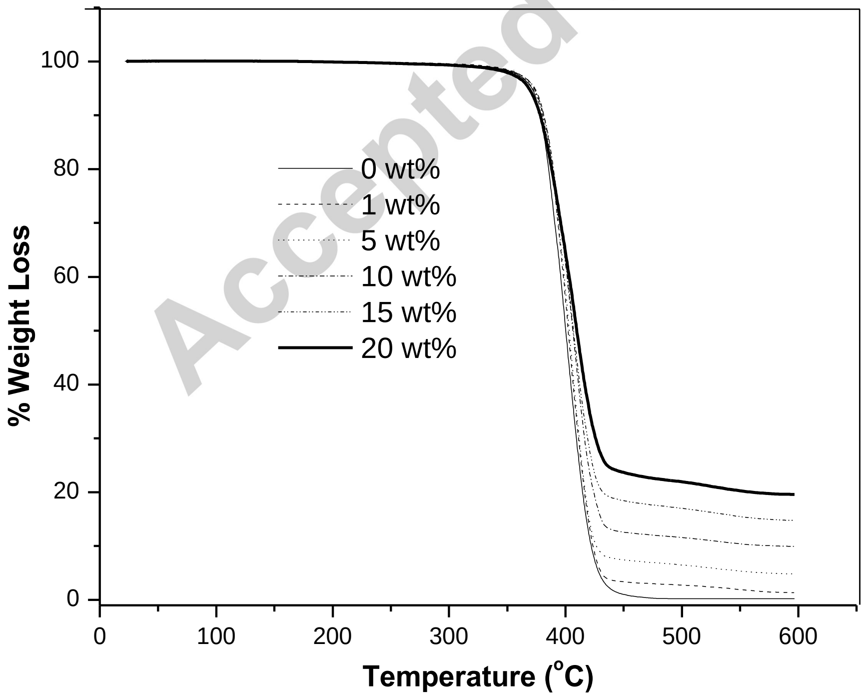

Figure 8. TGA analysis of cycloaliphatic epoxy filled silica nanoparticles at various filler contents under N_2 atmosphere from 25 ^{o}C to 600 ^{o}C with heating rate of 10 ^{o}C/min.

3.6 Fracture toughness

Fracture toughness is a measure of the ability of a material to resist the growth of pre-existing cracks or flaws. The improvement of the fracture toughness of the DGEBF and cycloaliphatic epoxies due to the silica nanoparticles was observed as shown in Fig. 9. The increase in fracture toughness with silica nanoparticles with these two systems indicates enhanced crack growth resistance over that of the neat epoxy. It is clearly shown that the DGEBF resin, with 20 wt.% of silica nanoparticles, and the cycloaliphatic resin, with 15 wt.% of silica nanoparticles, give the highest improvements in fracture toughness of the nanocomposites. Beyond these silica nanoparticle concentrations, the fracture toughness appears to either remain constant or slightly decrease.

The improvement in facture toughness when rigid nanofillers are added into a polymer matrix has been reported in many studies [34, 38, 39]. The high stress concentration in front of the tapped, natural crack within the neat resin is changed into a more uniform stress distribution due to the fine distribution of the nanoparticles, thus enhancing the toughness of the system. The enhanced toughness in epoxy modified silica nanoparticles is due to the interaction between the nanoparticles and polymer chains at the interface, leading to energy-dissipating toughening mechanisms. With increasing filler content, the interface area increases which should result in a substantially improved fracture toughness. However, the current study shows that at high wt.% of silica particles, the toughening effect plateaus or even slightly decreases. The K_{IC} profile follows where the fracture behavior can be controlled by the presence of the interface structures at low filler content. However, once the silica nanoparticle content increases and reaches a critical value, the fracture toughness remains constant.

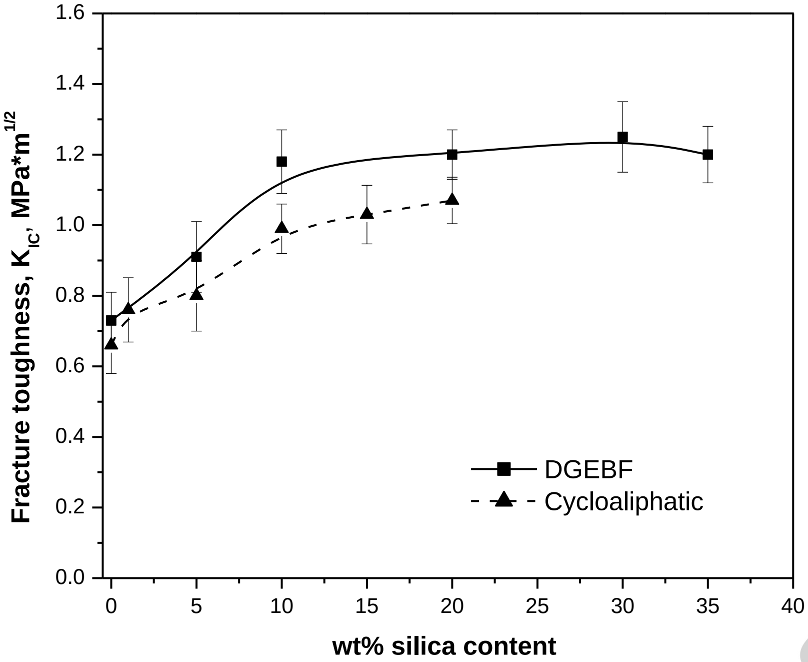

Figure 9. Fracture toughness of DGEBF and cycloaliphatic epoxies as a function of silica particle content.

3.7 Moisture absorption

The moisture absorption behavior of the epoxy/silica nanocomposites (starting from a dry sample and normalized by equal sample sizes) is measured as the weight gain% as a function of time. Diffusion studies at 85^{o}C and 85% relative humidity (RH) were used for all the epoxy formulations. The percent moisture content or percent weight gain, M, was measured as a function of time by the following equation:

$$M = M(t) = \frac{wt\ of\ moist\ material - wt\ of\ dry\ material}{wt\ of\ dry\ material} * 100\% \qquad (7)$$

The percent moisture content as a function of time (M_t) can be analyzed using Fick's second law [40]:

$$M_t = G(M_\infty - M_i) + M_i \qquad (8)$$

$$G = 1 - \frac{8}{\pi^2}\sum_{j=0}^{\infty}\frac{exp\left[-(2j+1)^2\pi^2(\frac{D_t}{b^2})\right]}{(2j+1)^2} \qquad (9)$$

where M_i is the initial percentage of moisture content in the sample and M_∞ is the percentage of moisture content at the equilibrium. The diffusivity can be estimated by plotting percent moisture uptake versus square root of time. The diffusion coefficient (*D*) can be calculated by the following equation:

$$D = \pi \left(\frac{sb}{4M_\infty}\right)^2 \tag{9}$$

where *s* is the slope of the initial linear portion of the plot and *b* is the sample thickness.

The moisture uptake plots for 0-35 wt.% silica nanoparticles filled DGEBF and 0-20 wt.% silica nanoparticle filled cycloaliphatic epoxies are depicted in Figs. 10 and 11, respectively. It is shown that for both systems, initially the rate or slope of absorption is high and increases linearly with time. As the material becomes saturated, moisture content levels off (slope approaches zero) to a final weight gain% at longer times. Furthermore, the moisture uptake is strongly affected by the different concentrations of the silica nanoparticles for both the DGEBF and cycloaliphatic epoxies, where higher filler content lowers the moisture uptake, as reflected by M_∞ listed in Table 4. As a result, the lower moisture absorption with higher silica nanoparticle content is particularly attractive for applications such as underfill epoxy resins. This improved moisture behavior is due to the increase of surface contact between filler and polymers as the amount of silica nanoparticles increases. The moisture absorption into the epoxy is also strongly controlled by diffusional effects. As the diffusion pathway for the moisture becomes longer with fillers acting as impenetrable roadblocks, the diffusion through the polymer is slower, resulting in a lower diffusion coefficient. The diffusion coefficients (*D*) of all the epoxy systems are listed in Table 4 and reveal that *D* decreases with increasing silica nanoparticle content for both DGEBF and cycloaliphatic epoxy systems. Consistent with the moisture absorption, *D* decreases with increasing filler content due to the larger surface contact of the fillers, which allows for less diffusion of the moisture through the epoxies.

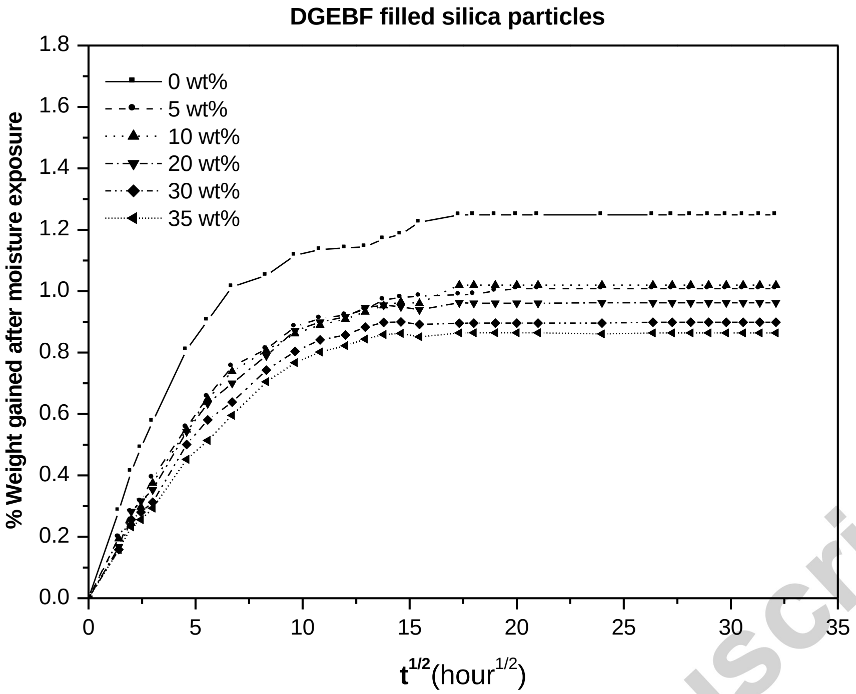

Figure 10. Moisture uptake results as a function of time at 85°C/85%RH for filled DGEBF epoxy systems.

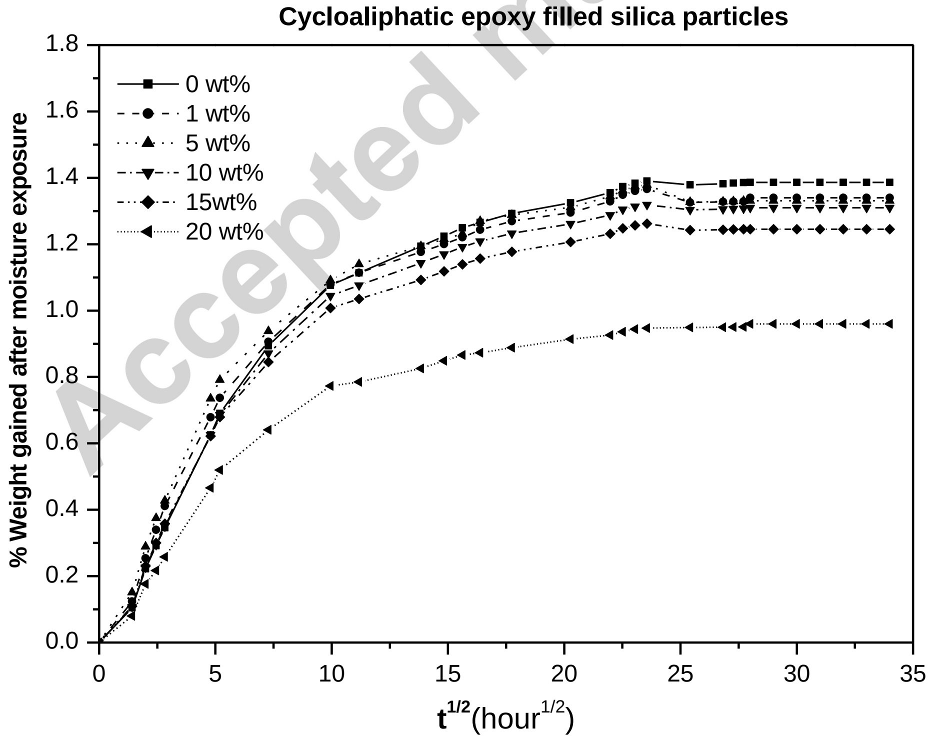

Figure 11. Moisture uptake results as a function of time at 85°C/85%RH for filled cycloaliphatic epoxy systems.

Table 4. Saturation mass and diffusion coefficients of all epoxy systems.

Epoxy System	Wt % Fillers	M_∞	D x 10^6 (cm^2/sec)
DGEBF	0	1.25±0.03	4.77
	5	1.08±0.02	3.89
	10	1.03±0.01	3.45
	20	0.96±0.02	3.44
	30	0.88±0.01	3.29
	35	0.84±0.02	2.64
Cycloaliphatic	0	1.39±0.02	0.563
	1	1.37±0.02	0.555
	5	1.32±0.03	0.538
	10	1.29±0.01	0.523
	15	1.20±0.01	0.519
	20	0.94±0.02	0.467

4. Conclusions

The effect of the addition of silica nanoparticles to two different epoxy systems was investigated for stiffness, CTE, thermal stability, and moisture absorption, which are all important properties for applications such as underfill epoxy. The addition of silica nanoparticles reduced the CTE for the modified DGEBF and cycloaliphatic epoxy resins and increased the stiffness, thermal stability, and fracture toughness. For thermal stability, the T_d of the DGEBF epoxy with addition of silica nanoparticles was found to be higher than the neat resin, indicating a higher decomposition temperature with fillers and better thermal stability, and also, the T_d improved with higher filler concentration. The T_d of the cycloaliphatic epoxy, on the other hand, increased with fillers up to 10 wt.%, then decreased slightly above 15 wt.% of silica nanoparticles due to a decrease in crosslink density. This study also revealed that moisture absorption was strongly affected by the different concentrations of the nanoparticles for both DGEBF and cycloaliphatic epoxy systems where a lower and more favorable moisture uptake was achieved with increasing silica nanoparticle content and where the rate of diffusion was controlled by the presence of fillers (diffusion coefficient, *D*, decreased with increasing silica nanoparticles content). Furthermore, the highest fracture toughness was achieved with approximately 20 wt.% and 15 wt.% of silica nanoparticles in the DGEBF and cycloaliphatic epoxy resins, respectively. Lastly, for the theoretical models used to predict the experimental results, the Kerner model was found to predict the CTE well, however, the Halpin-Tsai model was found to only predict the modulus well for selected epoxies, such as the modified cycloaliphatic epoxy, while being limited for other systems due to the lack of accounting for particle agglomeration and particle-particle interactions at the nanoscale level.

5. Acknowledgements

This work was supported by the Kasetsart University Research and Development Institute (KURDI), the Faculty of Engineering at Kasetsart University, and the Institutional Research Grant (grant no. IRG5980004) from the Thailand Research Fund. Support from Center for Polymer Science and Engineering at Lehigh University is also acknowledged.

6. References

[1] Brostow, W., Goodman, S.H., Wahrmund, J., 2014. Handbook of Thermoset Plastics (Third Edition), edited by Hanna Dodiuk and Sidney H. Goodman, William Andrew Publishing, Boston. 8, 191-252.

[2] Wu, P.X., Zhang, L.C., 1996. Polymer Blending Modification; China Light Industry Press: Beijing, China.

[3] Prolongo, S.F., Rosario, G.D., Ureña, A., 2006. Comparative study on the adhesive properties of different epoxy resins. Int. J. Adhes. Adhes. 26, 125-132.

[4] Pearson, R.A., Yee, A.F., 1993. Toughening mechanisms in thermoplastic-modified epoxies: 1. Modification using poly(phenylene oxide). Polymer. 34, 3658-3670.

[5] Zhou H., Liu H-Y., Zhou H., Zhang Y., Gao X., Mai Y-W., 2016. On adhesive properties of nano-silica/epoxy bonded single-lap joints, Materials & Design. 95, 212-218.

[6] Ilyin, S.O., Brantseva, T.V., Gorbunova. I.Yu., Antonov, S.V., Korolev, Yu.M., Kerber, M.L., 2015. Epoxy reinforcement with silicate particles: Rheological and adhesive properties – Part I: Characterization of composites with natural and organically modified montmorillonites. Int. J. Adhes. Adhes. 61, 127–136.

[7] Hsieh T.H., Kinloch A.J., Masani K, Taylor A.C., Sprenger S. 2010. The mechanisms and mechanics of the toughening of epoxy polymers modified with silica nanoparticles. Polymer 2010: 51, 6284-6294.

[8] Bray, D.J., Dittanet, P., Guild, F.J., Kinloch, A.J., Masania, K., Pearson, R.A., Taylor, A.C., 2013. The modelling of the toughening of epoxy polymers via silica nanoparticles: The effects of volume fraction and particle size. Polymer. 54, 7022-7032.

[9] Cowling, M.J., Smith, E.M., Hashin, S.A., Winkle, I.E., 1989. Performance of adhesively bonded steel connections for marine structure. Proceedings of the EVALMAT. 89, 827–834.

[10] Davis, M., Bond, D., 1999. Principles and practices of adhesive bonded structural joints and repairs. Int. J. Adhes. Adhes. 19, 91–105.

[11] Kerner, E.H., 1956. Elastic and thermoelastic properties of composite media. Proc. Phys. Soc. B. 69, 808-813.

[12] Nielsen, L.E., 1970. Generalized equation for the elastic moduli of composite materials. Applied Physics. 41, 4626-4627.

[13] Orrhede, M., Tolani, R., Salama, K., 1996. Elastic constants and thermal expansion of aluminum SiC metal matrix composites. Nondestructive Evaluation. 8(I), 23-37.

[14] Shin, D.K., Lee, J.J., 1998. Effective material properties and thermal stress analysis of epoxy molding compound in electronic packaging. IEEE Transactions on component, packaging, and manufacturing technology B. 21, 413-421.

[15] Mori, T., Tanaka K., 1973. Average stress in matrix and average elastic energy of materials with misfitting inclusions. Acta Metall. 21, 571-574.

[16] Halpin, J.C., 1969. Stiffness and expansion estimates for oriented short fiber composites. J. Compos. Mater. 3, 732-734.

[17] Jumahat, A., Soutis, C., Jones, F.R., Hodzic, A., 2012. Compressive behaviour of nanoclay modified aerospace grade epoxy polymer. Plast. Rubber. Compos. 41, 225-232.

[18] Arasteh R., Omidi M., Rousta A.H.A., Kazerooni H., 2011. A study on effect of waviness on mechanical properties of multi-walled carbon nanotube/epoxy composites using modified Halpin-Tsai Theory. J. Macromol. Sci. Part B: Phys. 50, 2464-2480.

[19] Han, J.T., Cho, K. 2006. Nanoparticle-induced enhancement in fracture toughness of highly loaded epoxy composites over a wide temperature range. J. Mater Sci. 41, 4239-4245.

[20] Tandon, G.P., Weng, G.J., 1984. The effect of aspect ratio of inclusions on the elastic properties of unidirectionally aligned composites. Polym Compos. 5, 327-333.

[21] Vo, H.T., Todd, M., Shi, F.G., Shapiro, A.A., Edwards, M., 2001. Towards model-based engineering of underfill materials: CTE modeling. Microelectronics. 32, 331-338.

[22] Mcadams B.J., 2005. Understanding adhesion issues at underfill/passivation interfaces. PhD dissertation, Lehigh University.

[23] Hertzberg, R.W., 1989. Deformation and fracture mechanics of engineering materials. (Third Edition) John Wiley & Sons, New York.

[24] Sprenger S., 2013. Epoxy resin composites with surface-modified silicon dioxide nanoparticles: A review, J. App. Polym. Sci. 130,1421-1428.

[25] Case S.L., Ward T.C., 2003. Physical properties of a bisphenol-F epoxy containing a silica filler treated with silane coupling agents, J. Adhes. 79, 105-121.

[26] Zhang, H., Zhang, Z., Friedrich, K., Eger, C., 2006. Property improvements of in-situ epoxy nanocomposites with reduced interparticle distance at high nanosilica content. Acta Mater. 54, 1833-1842.

[27] Wong, C.P., Bollampally, R.S., 1999. Thermal conductivity, elastic modulus, and coefficient of thermal expansion of polymer composites filled with ceramic particles for electronic packaging. J. Appl. Polym. Sci. 74, 3396-3403.

[28] Dittanet, P., Pearson, R.A., 2013. Effect of bimodal particle size distribution on toughening mechanisms in silica nanoparticle filled epoxy resin. Polymer. 54, 1832-1845.

[29] Dittanet, P., Pearson, R.A., 2012. Effect of silica nanoparticle size on toughening mechanisms of filled epoxy. Polymer. 53, 1890-1905.

[30] Zhang, K., Chen, H.T., Chen, X., Chen, Z.M., Cui, Z.C., Yang, B., 2003. Monodisperse silica-polymer core-shell microspheres via surface grafting and emulsion polymerization. Micromol. Mater. Eng. 288, 380-385.

[31] Liu, Y.L., Hsu, C.Y., Wei, W.L., Jeng, R.J., 2003. Preparation and thermal properties of epoxy-silica nanocomposites from nanoscale colloidal silica. Polymer. 44, 5159–5167.

[32] Johnsen B.B., Kinloch A.J., Mohammed R.D., Taylor A.C., Sprenger S. 2007. Toughening mechanisms of nanoparticle-modified epoxy polymers. Polymer, 48, 530-541.

[33] Halpin J.C., Kardos J.L., 1976. The Halpin-Tsai equations: a review. J. Polym. Eng. Sci. 186, 344-352.

[34] Adachi T. Osaki M. Araki W. Kwon SC. 2008. Fracture toughness of nano- and micro-spherical silica-particle-filled epoxy composites. Acta Mater. 56, 2101-2109.

[35] Zhang, M.Q., Rong, M.Z., Yu, S.L., Wetzel, B., Friedrich, K., 2002. Effect of particle surface treatment on the tribological performance of epoxy based nanocomposites. Wear. 253, 1086-1093.

[36] Lee, T.M., Ma, C.C.M., 2005. Nonaqueous synthesis of nanosilica in epoxy resin matrix and thermal properties of their cured nanocomposites. J. Polym. Sci. Part A: Polym. Chem. 44, 757-768.

[37] The P.L., Jaafar M., Akil H.M., Seetharamu K.N., Wagiman A.N.R. Beh K.S., 2008. Thermal and mechanical properties of particulate fillers filled epoxy composites for electronic packaging application, Polym. Adv. Technol. 19, 308-315.

[38] Zhou H., Liu H-Y., Zhou H., Zhang Y., Gao X., Mai Y-W., 2016. On adhesive properties of nano-silica/epoxy bonded single-lap joints, Mater. Des. 95, 212-218.

[39] Tang Y., Ye L., Zhang Z., Friedrich K., 2013. Interlaminar fracture toughness and CAI strength of fibre-reinforced composites with nanoparticles – A review. Comp. Sci. Tech. 86, 26–37.

[40] Sperling LH. 2006. Introduction to physical polymer science (4th edition) John Wiley & Sons, New York, 173-181.